Study of stability of dc glow discharges with the use of Comsol Multiphysics software

2011 J. Phys. D: Appl. Phys. 44 415203

(http://iopscience.iop.org/0022-3727/44/41/415203)

IOP PUBLISHING JOURNAL OF PHYSICS D: APPLIED PHYSICS

J. Phys. D: Appl. Phys. **44** (2011) 415203 (10pp) doi:10.1088/0022-3727/44/41/415203

Study of stability of dc glow discharges with the use of Comsol Multiphysics software

P G C Almeida, M S Benilov and M J Faria

Departamento de Física, Universidade da Madeira, Largo do Município, 9000 Funchal, Portugal

Received 25 July 2011, in final form 24 August 2011
Published 27 September 2011
Online at stacks.iop.org/JPhysD/44/415203

Abstract

Stability of different axially symmetric modes of current transfer in dc glow discharges is investigated in the framework of the linear stability theory with the use of Comsol Multiphysics software. Conditions of current-controlled microdischarges in xenon are treated as an example. Both real and complex eigenvalues have been detected, meaning that perturbations can vary with time both monotonically and with oscillations. In general, results given by the linear stability theory confirm intuitive concepts developed in the literature and conform to the experiment. On the other hand, suggestions are provided for further experimental and theoretical work.

(Some figures in this article are in colour only in the electronic version)

1. Introduction

Investigation of stability of stationary configurations is particularly important in cases where different configurations are possible and one needs to determine which of them can be realized. Such is the case with current transfer to cathodes of dc glow and arc discharges. It was known long ago that current transfer to glow cathodes can occur in the abnormal mode and in the normal mode, e.g. [1]. Modes with more than one spot have been observed on cathodes of non-self sustained dc glow discharges [2–4] and in dc glow microdischarges [5–9]. A diffuse mode and a mode with a spot occur on cathodes of high-pressure arc discharges ([10, 11]; see [12] for further references).

It was hypothesized quite some time ago [13–15] that different modes of current transfer to cathodes of dc arc and glow discharges are described by multiple steady-state solutions that should exist at the same discharge current. Note that the existence of multiple steady-state solutions is an inherent feature of the theory of nonlinear dissipative systems admitting stationary self-organized patterns. Over the last decade, such multiple solutions have been computed in the theory of current transfer to cathodes of high-pressure arc discharges (e.g. review [16]) and have served as a basis of the generally accepted theory. Recently, such multiple steady-state solutions were computed also for dc glow discharges [17, 18] and were found to describe both the normal mode and modes with multiple spots similar to those observed in dc glow microdischarges [5–9].

The patterns of multiple steady-state solutions found for dc glow discharges and for cathodes of high-pressure arc discharges are similar in many aspects [19]. In particular, the theory indicates that in both cases current is distributed over the cathode surface more or less uniformly at higher currents and is localized in one or more regions (spots) occupying only a fraction of the cathode surface at lower currents. This is indeed what is observed in the experiment; note that the diffuse and spot modes on arc cathodes represent analogues of the abnormal and normal modes on glow cathodes.

However, the patterns of modes observed in the experiment on glow and arc cathodes have also important differences: modes with more than one spot observed on glow cathodes have not been observed on arc cathodes; axially symmetric current distributions on planar circular cathodes have not been observed on arc cathodes but seem to have been observed in glow discharges (the upper-left image in figure 3 of [5] and the middle image in figure 4 of [9]). Given that the patterns of multiple steady-state solutions are similar, one should presume that these differences are caused by substantially different properties of stability of these solutions. There is another experimental fact supporting this hypothesis: temporal oscillations of the discharge voltage can develop in the course of transition from the Townsend discharge to the normal mode of glow discharge (e.g. [20–22]), while

no such oscillations nor oscillations of luminosity of the cathode surface have been observed in high-pressure arcs. It is interesting to note for comparison that no observations have been reported of oscillations in the course of transitions both from the abnormal mode of glow discharge to the normal mode or a mode with multiple spots and from the diffuse mode on a high-pressure arc cathode to the spot mode.

Main features of stability of current transfer to arc cathodes have been investigated in the framework of the linear stability theory both analytically [23] and numerically [24]. On the other hand, no investigations of stability of dc glow discharge on the whole have apparently been reported, although there are many works dedicated to investigation of stability of the positive column (e.g. books [1, 25], papers [26, 27] are further examples); one should mention also an investigation of stability of 1D Townsend discharge against 1D perturbations [20]. In part, this is explained by the fact that most researchers working in the field compute steady-state solutions by means of simulating temporal evolution of the discharge with the use of a non-stationary code: one could think that temporal evolution cannot lead to an unstable steady state and therefore all stationary solutions obtained by means of a non-stationary code are stable. However, the latter is only true with respect to perturbations having the same symmetry to which the code is adjusted. For example, an axially symmetric (2D) steady-state solution calculated by means of a non-stationary 2D code is stable against 2D perturbations but is not necessarily stable against 3D perturbations, which are frequently the most dangerous ones.

An adequate tool for investigation of stability of stationary configurations is the linear stability theory. In addition to indicating whether a given stationary state is stable or unstable, this theory allows one to find states where one of the perturbation modes is stationary. Such states represent points of bifurcation of steady-state modes and play an important role in computing [17, 18] and understanding [19] different modes of operation of dc glow discharges. The Comsol Multiphysics software is a convenient tool for numerical solution of the eigenvalue boundary-value problem appearing in the framework of the linear stability theory. For example, this software was successfully employed for investigation of stability of current transfer to arc cathodes [24].

This paper is concerned with a numerical investigation of stability of axially symmetric steady-state modes of dc glow discharges in the framework of the linear stability theory with the use of Comsol Multiphysics, the principal objective being to find out main features of stability of dc glows as predicted by the linear stability theory and compare them with the common knowledge based on the experiment and intuitive considerations (e.g. [1]). Points of bifurcation of steady-state modes are calculated as well. Calculation results are given for conditions of current-controlled microdischarges in xenon.

The outline of the paper is as follows. A mathematical model is introduced in section 2. Relevant aspects of numerical solution with the use of Comsol Multiphysics are discussed in section 3. Numerical results on stability of different 2D steady-state modes are given and analysed in sections 4 and 5. Concluding remarks are given in section 6.

2. The model

Self-organization in cold glow and glow-like gas discharges is usually simulated by means of a basic glow discharge model assuming a single ion species, direct electron impact ionization, secondary electron emission by ion impact and electron kinetic and transport coefficients being functions of the local electric field. It was shown that this model can reproduce many features observed experimentally and allows one to understand pattern formation in DBDs [28–31] and dc glow discharges [17, 18], formation and propagation of filamentary plasma arrays in high-power microwave breakdown at atmospheric pressure [32, 33]. In [34], self-organized patterns on dc glow cathodes have been studied by means of a more realistic model of dc glows, which is in the spirit of models usually employed for detailed simulation of microdischarges in the absence of self-organization [35–40] and which accounts for two ionic species, several ionization channels, non-equilibrium population of excited states and comprises an energy equation for the electrons with appropriate boundary conditions (similar to those [41]). It was found that the effect of chemistry and non-locality of electron kinetic and transport coefficients does not cause qualitative changes in self-organization, which explains why the use of the basic model in simulations of self-organization has been successful. The basic model is used also in this work.

2.1. System of equations

The system of equations comprises equations of conservation of a single ion species (molecular ions) and the electrons, transport equations for the ions and the electrons written in the drift–diffusion local-field approximation and the Poisson equation:

$$\frac{\partial n_\mathrm{i}}{\partial t} + \nabla \cdot \boldsymbol{J}_\mathrm{i} = w, \qquad \boldsymbol{J}_\mathrm{i} = -D_\mathrm{i}\nabla n_\mathrm{i} - \mu_\mathrm{i} n_\mathrm{i} \nabla\varphi, \tag{1}$$

$$\nabla \cdot \boldsymbol{J}_\mathrm{e} = w, \qquad \boldsymbol{J}_\mathrm{e} = -D_\mathrm{e}\nabla n_\mathrm{e} + \mu_\mathrm{e} n_\mathrm{e} \nabla\varphi, \tag{2}$$

$$\varepsilon_0 \nabla^2 \varphi = -e(n_\mathrm{i} - n_\mathrm{e}), \tag{3}$$

where

$$w = n_\mathrm{e}\alpha\mu_\mathrm{e}E - \beta n_\mathrm{e} n_\mathrm{i}. \tag{4}$$

Here n_i, n_e, $\boldsymbol{J}_\mathrm{i}$, $\boldsymbol{J}_\mathrm{e}$, D_i, D_e, μ_i and μ_e are number densities, densities of transport fluxes, diffusion coefficients and mobilities of the ions and electrons, respectively, α is Townsend's ionization coefficient, β is the coefficient of dissociative recombination, φ is scalar potential, $E = |\nabla\varphi|$ is modulus of the electric field, ε_0 is the permittivity of free space, e is the elementary charge, and t is time.

The only non-stationary term in the above system of equations appears in the equation of conservation of the ions, first equation in (1), and the electric field is expressed in terms of scalar potential without involving the vector potential. These approximations are justified if stability of the discharge is governed by perturbations with frequency (or growth rate) of the order of the inverse characteristic time of ion drift, τ_i^{-1}. (The characteristic time of ion drift may be defined in the simplest case as $\tau_\mathrm{i} = h^2/\mu_\mathrm{i}^{(0)}U^{(0)}$, where h is the interelectrode

gap, U is the discharge voltage and the upper index (0) denotes a characteristic value. τ_i is of the order of 1 μs under conditions of interest for this work.)

One of the channels of development of perturbations in the discharge, namely, perturbation of the electric field by perturbations of the ion density, is effectively switched off on frequencies substantially higher than τ_i^{-1}, where the ion density is not perturbed. Therefore, one can expect that the enhancement of perturbations on frequencies substantially exceeding τ_i^{-1} is indeed less likely than that on frequencies of the order of τ_i^{-1}. In order to check this reasoning, calculations have been performed with account of the non-stationary terms both in the ion and electron conservation equations, although still neglecting perturbation of the electric field due to perturbations of the vector potential. It has been found that the account of the non-stationary term in the electron conservation equation results in appearance of a high-frequency part of the spectrum; the spectrum of perturbations with frequencies of the order of τ_i^{-1} is not affected appreciably and it is these perturbations that can be growing, in agreement with the above reasoning. Note that computation of a spectrum containing a high-frequency part by means of an approach described below and based on the Comsol Multiphysics software requires significantly more computer time.

It will be convenient for the purposes of this work to rewrite the first equations in (1) and (2) in the following form:

$$\frac{\partial n_i}{\partial t} - \nabla \cdot (D_i \nabla n_i) - \nabla (\mu_i n_i) \cdot \nabla \varphi + \frac{e}{\varepsilon_0} \mu_i n_i (n_i - n_e) = w, \tag{5}$$

$$-\nabla \cdot (D_e \nabla n_e) + \nabla (\mu_e n_e) \cdot \nabla \varphi - \frac{e}{\varepsilon_0} \mu_e n_e (n_i - n_e) = w. \tag{6}$$

Numerical results reported in this work refer to a discharge in xenon under the pressure of 30 Torr. The transport and kinetics coefficients are the same as in [17]; in particular, constant values are assumed for the transport and dissociative recombination coefficients.

2.2. Boundary conditions

Numerical results reported in this work refer to a microdischarge in a cylindrical tube of a radius $R = 1.5$ mm and of a height $h = 0.5$ mm with metal electrodes. Let us introduce cylindrical coordinates (r, ϕ, z) with the origin at the centre of the cathode and the z-axis coinciding with the axis of the tube. Boundary conditions at the cathode ($z = 0$) and anode ($z = h$) are written in the conventional form

$$z = 0\colon \ \frac{\partial n_i}{\partial z} = 0, \qquad J_{ez} = -\gamma J_{iz}, \qquad \varphi = 0; \tag{7}$$

$$z = h\colon \ n_i = 0, \qquad \frac{\partial n_e}{\partial z} = 0, \qquad \varphi = U. \tag{8}$$

The subscripts z and r here and further denote axial and, respectively, radial projections of corresponding vectors. The meaning of these boundary conditions is well known: diffusion fluxes of the attracted particles are neglected compared with drift; the normal flux of the electrons emitted by the cathode is related to the flux of incident ions in terms of the effective secondary emission coefficient γ, which is assumed to characterize all mechanisms of electron emission (due to ion, photon and excited atom bombardment); density of ions vanishes at the anode; electrostatic potentials of both electrodes are given.

The following boundary conditions are applied at the (dielectric) wall of the tube:

$$r = R\colon \ e(J_{ir} - J_{er}) - \varepsilon_0 \frac{\partial^2 \varphi}{\partial t \, \partial r} = 0, \qquad n_i = n_e = 0. \tag{9}$$

These boundary conditions are similar to those used by other authors (e.g. [42, 43]). The first boundary condition means zero of the radial component of the total electric current density, which implies neglect of the radial component of the displacement current inside the dielectric wall. The second boundary condition is written under the assumption that all ions and electrons coming to the wall are absorbed, with eventual neutralization and return of the appearing neutral atoms into the plasma.

The discharge is assumed to be current-controlled. Therefore, the discharge current or, equivalently, the average density of net electric current in the direction from anode to cathode,

$$\langle j \rangle = -\frac{1}{\pi R^2} \int_0^{2\pi} \int_0^R \left[e(J_{iz} - J_{ez}) - \varepsilon_0 \frac{\partial^2 \varphi}{\partial t \, \partial z} \right] r \, \mathrm{d}r \, \mathrm{d}\phi, \tag{10}$$

is treated as a given parameter. Accordingly, the discharge voltage U is found in the course of simulations.

The above problem, when applied to treatment of stationary states, admits an axially symmetric (2D) solution, $F = F(r, z)$ (here F is any of the quantities n_i, n_e and φ) which exists at all discharge currents. This solution is designated the fundamental mode. Under certain conditions, the problem also admits other 2D solutions, which exist in a limited current range and represent a closed loop, and 3D solutions, which also exist in a limited current range. In this work, stability is studied of 2D steady states belonging to both fundamental and non-fundamental modes.

2.3. Eigenvalue problem describing stability

Perturbations of 2D stationary states can be 2D or 3D. In the framework of the conventional formalism of the linear stability theory, a solution to the problem (5), (6), (3), (4), (7)–(10) is sought as sum of a steady-state solution and small perturbations with exponential time dependence. Taking into account that the 3D perturbations are harmonic with respect to the azimuthal angle ϕ, one can write

$$n_{i,e}(r, \phi, z, t) = n_{i0,e0}(r, z) + \mathrm{e}^{\lambda t} n_{i1,e1}(r, z) \cos m\phi + \cdots, \tag{11}$$

$$\varphi(r, \phi, z, t) = \varphi_0(r, z) + \mathrm{e}^{\lambda t} \varphi_1(r, z) \cos m\phi + \cdots, \tag{12}$$

$$U(t) = U_0 + \mathrm{e}^{\lambda t} U_1 + \cdots. \tag{13}$$

Here the first term on the right-hand side (rhs) of each expansion represents a solution describing the stationary state stability which is being studied, the second term represents a perturbation of this state, λ is the rate of growth of the perturbation and $m = 0, 1, 2, \ldots$. If $m = 0$, the perturbation being considered is 2D. If $m = 1, 2, \ldots$, the perturbation is 3D with period in ϕ equal to $2\pi/m$.

Substituting expansions (11)–(13) into equations (5), (6), (3), (4), boundary conditions (7)–(9) and equation (10), linearizing, and equating linear terms, one obtains

$$\lambda n_{i1} - D_i \nabla^2 n_{i1} + D_i \left(\frac{m}{r}\right)^2 n_{i1} - \mu_i (\nabla n_{i1} \cdot \nabla \varphi_0 + \nabla n_{i0} \cdot \nabla \varphi_1) + \mu_i \frac{e}{\varepsilon_0} [n_{i1}(n_{i0} - n_{e0}) + n_{i0}(n_{i1} - n_{e1})] = w_1, \quad (14)$$

$$-D_e \nabla^2 n_{e1} + D_e \left(\frac{m}{r}\right)^2 n_{e1} + \mu_e (\nabla n_{e1} \cdot \nabla \varphi_0 + \nabla n_{e0} \cdot \nabla \varphi_1) - \mu_e \frac{e}{\varepsilon_0} [n_{e1}(n_{i0} - n_{e0}) + n_{e0}(n_{i1} - n_{e1})] = w_1, \quad (15)$$

$$-\nabla^2 \varphi_1 + \left(\frac{m}{r}\right)^2 \varphi_1 = \frac{e}{\varepsilon_0} (n_{i1} - n_{e1}); \quad (16)$$

$$z = 0\colon \frac{\partial n_{i1}}{\partial z} = 0, \quad -D_e \frac{\partial n_{e1}}{\partial z} + \mu_e \left(n_{e1} \frac{\partial \varphi_0}{\partial z} + n_{e0} \frac{\partial \varphi_1}{\partial z}\right) = \gamma \mu_i \left(n_{i1} \frac{\partial \varphi_0}{\partial z} + n_{i0} \frac{\partial \varphi_1}{\partial z}\right), \quad \varphi_1 = 0; \quad (17)$$

$$z = h\colon n_{i1} = 0, \quad \frac{\partial n_{e1}}{\partial z} = 0, \quad \varphi_1 \cos m\phi = U_1; \quad (18)$$

$$r = R\colon e\left(-D_i \frac{\partial n_{i1}}{\partial r} + D_e \frac{\partial n_{e1}}{\partial r}\right) - \varepsilon_0 \lambda \frac{\partial \varphi_1}{\partial r} = 0, \quad n_{i1} = n_{e1} = 0; \quad (19)$$

$$\delta_{m0} \int_0^R \left[e\left(- D_i \frac{\partial n_{i1}}{\partial z} - \mu_e n_{e1} \frac{\partial \varphi_0}{\partial z} - \mu_e n_{e0} \frac{\partial \varphi_1}{\partial z}\right) - \varepsilon_0 \lambda \frac{\partial \varphi_1}{\partial z}\right]_{z=h} r \, \mathrm{d}r = 0. \quad (20)$$

Here

$$w_1 = \mu_e \left[n_{e1} \, \alpha|_{E_0} \, E_0 + \frac{n_{e0}}{E_0} \frac{\mathrm{d}(\alpha E)}{\mathrm{d}E}\bigg|_{E_0} \nabla \varphi_0 \cdot \nabla \varphi_1 \right] - \beta (n_{i0} n_{e1} + n_{e0} n_{i1}). \quad (21)$$

It should be stressed that although equations (14)–(16) are written in terms of ∇, there are no azimuthal derivatives in these equations since n_{i0}, n_{i1}, n_{e0}, etc are functions only of r and z. Equation (20) reflects the assumption that the discharge current is maintained unperturbed by the external circuit (the limiting case of a very high ballast or, equivalently, a current-controlled discharge) and Kronecker delta δ_{m0} on the left-hand side (lhs) originates in integration over ϕ. For definiteness, the discharge current is evaluated at the anode.

In the case $m \neq 0$, equation (20) is satisfied trivially: perturbations which are harmonic in ϕ do not perturb discharge current. On the other hand, the last boundary condition in (18) cannot be satisfied in the case $m \neq 0$ unless both sides vanish. Therefore, the last boundary condition in (18) in the case $m \neq 0$ is equivalent to two relations: $\varphi_1(r, h) = 0$, $U_1 = 0$.

Equations (14)–(21) represent a linear eigenvalue problem, λ being the eigenvalue. By means of solving this problem for a given m, one will determine a set of eigenvalues λ (spectrum) associated with this m. By means of repeating this procedure for each m and joining the obtained spectra, one will find the whole spectrum of the stationary state being treated.

3. Numerical solution with Comsol Multiphysics

Commercial software Comsol Multiphysics also provides, in addition to stationary and non-stationary solvers, a powerful eigenvalue solver, which may be used for investigation of stability of stationary solutions. However, this requires a certain amount of care, as experience of investigation of stability of current transfer to thermionic cathode of high-pressure arc discharges [12, 24, 44] has shown.

A straightforward approach is to introduce the non-stationary equations of section 2.1 in the 3D geometry and then invoke for each value of the discharge current first the stationary solver, thus finding a solution describing the steady state corresponding to the current value being considered, and then the eigenvalue solver, thus finding spectrum of perturbations of this steady state.

Another approach consists in introducing the steady-state problem and the eigenvalue problem for perturbations separately. Of course, this approach requires more effort, because it involves a manual derivation and introduction of the perturbation problem instead of letting Comsol generate it. One of the advantages of this approach is the possibility of treating cases where the stationary state and its perturbations possess different symmetries; for example, this approach allowed an investigation of stability of 3D stationary states on axially symmetric cathodes of high-pressure arc discharges, which possess planar symmetry, against antisymmetric perturbations [44]. Another advantage appears in cases where the steady state is axially symmetric: it is natural to formulate the perturbation problem in 2D, as was done in section 2.3, and solve both the stationary and eigenvalue problems in the 2D geometry. In addition to a dramatic reduction in RAM and CPU time, this results in the elimination of difficulties originating in an extreme sensitivity of results of 3D stability calculations with respect to details of the steady state in the vicinity of the axis of symmetry [12].

The approach employed in this work for investigation of stability of axially symmetric stationary glow discharges may be viewed as a combination of the two above approaches. Terms involving derivatives with respect to ϕ on the lhs of each of equations (5), (6) and (3) are replaced with the following terms, respectively: $D_i(m/r)^2 n_i$, $D_e(m/r)^2 n_e$ and $(m/r)^2 \varphi$. Note that these terms are similar to those present in equations (14)–(16). The resulting non-stationary equations are introduced in Comsol as in the first above-described approach, but in the 2D geometry rather than in 3D. One sets

$m = 0$ before invoking the stationary solver and changes m to a desired value before invoking the eigenvalue solver. This approach offers the advantages of the second above-described approach while not requiring a manual introduction of the perturbation problem.

Note that when implemented on the same numerical mesh in Comsol Multiphysics versions 3.5a and 4.0a, the second above-described approach gives spectra which do not agree between themselves for some discharge currents in the case $m \neq 0$. Although considerable effort has been invested, this problem remained unsolved. On the other hand, spectra given by the third approach under both versions agree between themselves and also with the spectra given by the second approach under Comsol 3.5a.

In general, calculation of perturbations requires a more refined mesh than a calculation of stationary states: typically, from 2400 to 11 000 finite elements were necessary, depending on degree of non-uniformity of the state. Calculation of perturbations of a stationary state took from 5 s to 30 min on a PC with a 3.2 GHz processor, depending on the number of finite elements, on the order of magnitude of the value around which the spectrum is being sought (higher orders require more computer time), and on the number of eigenvalues that need to be found in order to make sure that the one with the biggest real part has not been missed.

4. Stability of the fundamental mode

In this section, results of numerical calculations of spectra of perturbations are reported and discussed for the fundamental (existing for all discharge currents) steady-state mode. In principle, for every stationary state belonging to this mode it is sufficient to find only the eigenvalue with the biggest real part; the state is stable if the latter is non-positive and unstable otherwise. However, it is useful to have information on all eigenvalues with positive real part for every stationary state. In particular, this information helps one to understand the results by means of analysing variation of the spectrum along the steady-state mode and comparing it with the usual pattern of perturbations of bistable nonlinear dissipative systems.

4.1. Numerical results

The dependence $U(\langle j \rangle)$ for the fundamental mode is shown in figure 1. Since the average current density $\langle j \rangle$ is proportional to the discharge current, this dependence may be called the current–voltage characteristic (CVC). Without going into details (see [17]), we note that the Townsend discharge and the subnormal discharge join through a Z-shape with turning points designated $a^{(3)}$ and $a^{(2)}$.

A large number of different perturbation modes have been found, some of them real and others complex. Complex perturbations exist in pairs with perturbations of each pair being complex conjugate and associated with eigenvalues which are complex conjugate as well, real perturbations are associated with real eigenvalues; a general property of linear eigenvalue problems with real coefficients. In order to distinguish between perturbation modes with the same m (i.e.

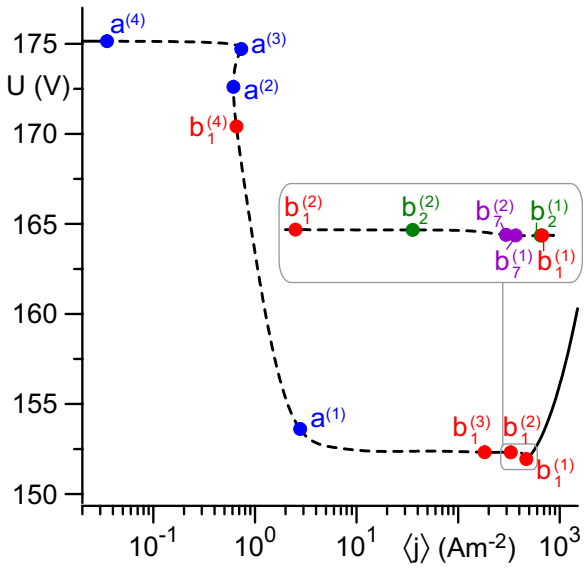

Figure 1. CVC of the fundamental mode. Solid: stable sections. Dashed: unstable sections. Circles: points of change in stability against a mode of real perturbations or against two complex conjugate modes.

with the same angular dependence $\cos m\phi$) but with different dependences on r and z, let us number such perturbation modes in the order of decrease in $\mathrm{Re}\,\lambda$ and designate this number by q. In the case of a pair of complex conjugate perturbations, the one associated with an eigenvalue with, say, positive imaginary part is counted first. Thus, each mode of perturbations will be identified by the corresponding numbers (m, q).

Switching of perturbations of different modes between decay and growth is illustrated by figures 1 and 2. At $\langle j \rangle \gtrsim 469\ \mathrm{A\,m^{-2}}$, real parts of the eigenvalues of all perturbation modes are negative and the discharge is stable. As $\langle j \rangle$ decreases, real parts of the eigenvalues increase and eventually $\mathrm{Re}\,\lambda$ of two complex conjugate perturbation modes with $m = 1$ becomes positive. This happens at $\langle j \rangle \approx 469\ \mathrm{A\,m^{-2}}$; state $b_1^{(1)}$. Note that the latter state belongs to the rising section of the CVC, however, it is quite close to the point of minimum $\langle j \rangle \approx 466\ \mathrm{A\,m^{-2}}$. As $\langle j \rangle$ decreases further, real parts of the eigenvalues of other perturbation modes turn positive. This happens in the order of increase of the value of m, hence the following perturbation modes to grow are two (complex conjugate) modes with $m = 2$ (at state $b_2^{(1)}$), then two modes with $m = 3$, two modes with $m = 4$, two modes with $m = 5$. After that, a real perturbation mode with $m = 6$ grows. Finally, a real perturbation mode with $m = 7$ grows (at state $b_7^{(1)}$). As $\langle j \rangle$ decreases further, real parts of the eigenvalues of all growing perturbation modes return to negative values. This happens in the order of decrease in m, hence the first perturbation mode to return to decaying is the real mode with $m = 7$ (at state $b_7^{(2)}$) and the last ones are two (complex conjugate) modes with $m = 2$ (at state $b_2^{(2)}$) and two modes with $m = 1$ (at $\langle j \rangle \approx 330\ \mathrm{A\,m^{-2}}$; state $b_1^{(2)}$).

Some growing 3D perturbations are real and other are complex. In addition, growing perturbations can switch between real and complex. Let us consider, for example, switching of the growing perturbations with $m = 1$ shown

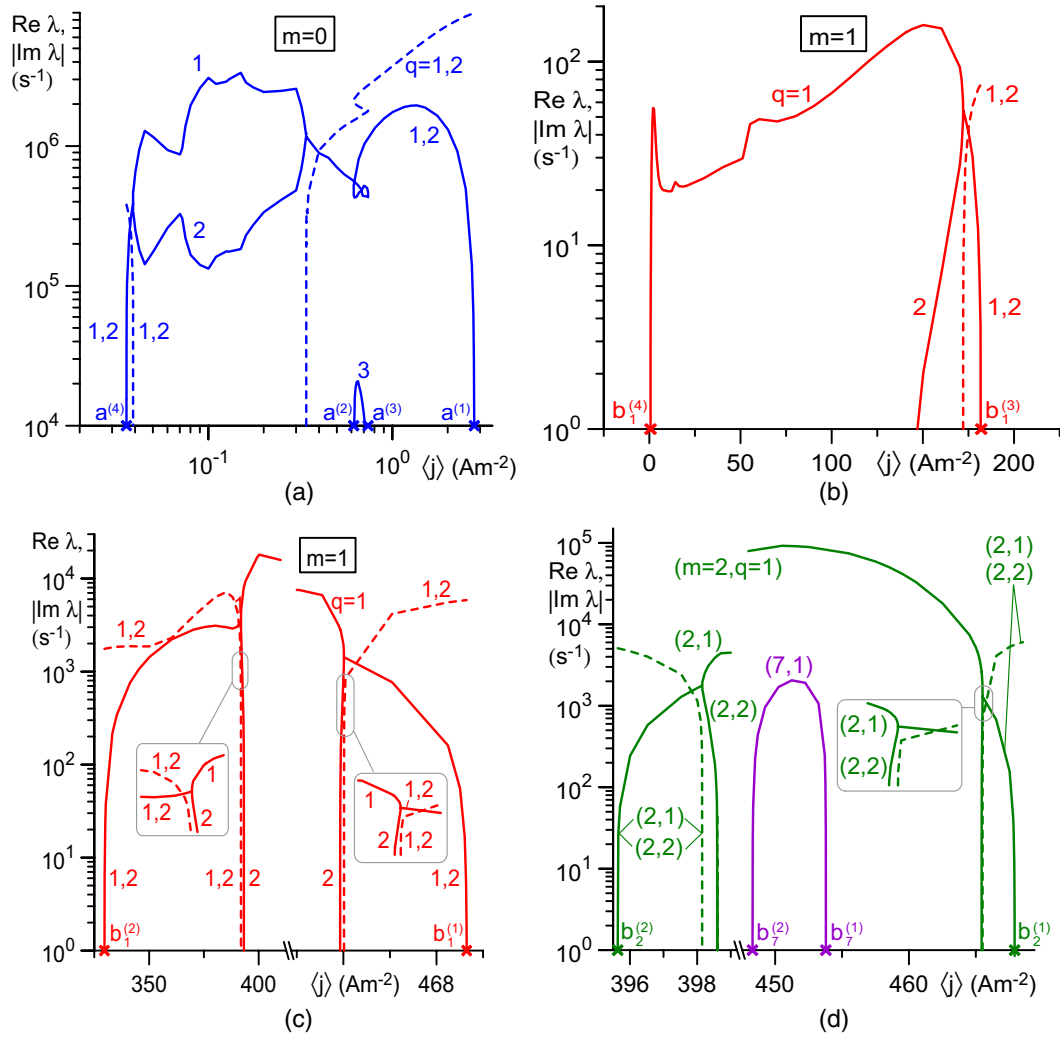

Figure 2. Eigenvalues of growing perturbations of stationary states belonging to the fundamental mode. Solid: real part of the eigenvalue. Dashed: modulus of the imaginary part. Crosses: values of $\langle j \rangle$ where stability changes against a mode of real perturbations or against two complex conjugate modes. (*a*) Axially symmetric perturbations. (*b*), (*c*) 3D perturbations with $m = 1$. (*d*) 3D perturbations with $m = 2, 7$.

in figure 2(*c*). Two complex conjugate perturbations with $m = 1$ turn to growing at the state $b_1^{(1)}$. However, $|\mathrm{Im}\,\lambda|$ rapidly decreases with decrease in current and vanishes at $\langle j \rangle \approx 466\,\mathrm{A\,m^{-2}}$: a switching to two real perturbations occurs. The eigenvalue of one of these perturbations (the one with $q = 2$) rapidly decreases and at $\langle j \rangle$ still very close to $466\,\mathrm{A\,m^{-2}}$ it vanishes, i.e. the perturbation is decaying. There is only one growing real perturbation mode with $m = 1$ at $393\,\mathrm{A\,m^{-2}} \lesssim \langle j \rangle \lesssim 466\,\mathrm{A\,m^{-2}}$. Another real perturbation (the one with $q = 2$) starts growing at $\langle j \rangle \approx 393\,\mathrm{A\,m^{-2}}$. The eigenvalue of the latter perturbation grows very fast and at $\langle j \rangle \approx 392\,\mathrm{A\,m^{-2}}$ becomes equal to the eigenvalue of the perturbation with $q = 1$. At smaller currents, the eigenvalues become complex conjugate; a switching from two real to two complex perturbations occurs. The latter perturbations start decaying at the state $b_1^{(2)}$.

As shown in figure 1, after having regained stability at state $b_1^{(2)}$ the discharge remains stable until state $b_1^{(3)}$ ($\langle j \rangle \approx 182\,\mathrm{A\,m^{-2}}$). Two (complex conjugate) modes with $m = 1$ start growing at the latter state; figure 2(*b*). (A theoretically interesting question is whether these are the same perturbation modes that returned to decay at the state $b_1^{(2)}$, however this question is not easy to answer because there are other decaying modes with similar eigenvalues and distributions between $b_1^{(2)}$ and $b_1^{(3)}$.) The perturbations turn real at $\langle j \rangle \approx 172\,\mathrm{A\,m^{-2}}$. One of these real perturbations returns to decaying at $\langle j \rangle \approx 141\,\mathrm{A\,m^{-2}}$ and the other at $\langle j \rangle \approx 0.66\,\mathrm{A\,m^{-2}}$ (state $b_1^{(4)}$).

However, the discharge does not return to stability at state $b_1^{(4)}$ since there are two growing complex perturbation modes with $m = 0$ at this state. These perturbations start growing at state $a^{(1)}$ ($\langle j \rangle \approx 2.8\,\mathrm{A\,m^{-2}}$), switch to being real at $\langle j \rangle \approx 0.34\,\mathrm{A\,m^{-2}}$, switch back to being complex at $\langle j \rangle \approx 40\,\mathrm{mA\,m^{-2}}$, and return to decay at state $a^{(4)}$ ($\langle j \rangle \approx 36\,\mathrm{mA\,m^{-2}}$); see figure 2(*a*).

One more perturbation mode, real perturbations with $m = 0$ and $q = 3$, turns to growing between turning points $a^{(2)}$ and $a^{(3)}$; figure 2(*a*).

For currents below $36\,\mathrm{mA\,m^{-2}}$, the discharge remains stable.

In terms of bifurcations, one can say that Hopf bifurcations occur at states $b_m^{(1)}$ with $m = 1, \ldots, 5$, states $b_m^{(2)}$ with $m = 1, 2, 3$, and states $b_1^{(3)}$, $a^{(1)}$, and $a^{(4)}$. Bifurcations of steady-state modes occur at states $b_m^{(1)}$ with $m = 6, 7$, states

$b_m^{(2)}$ with $m = 4, 5, 6, 7$, and state $b_1^{(4)}$: a 3D steady-state mode branches off from, or joins, the (2D) fundamental mode at each of these states. In addition, stationary bifurcations occur at every state where a real 3D perturbation with $q > 1$ switches between decaying and growing. Strictly speaking, steady-state bifurcations occur also at the turning points $a^{(2)}$ and $a^{(3)}$; however, these bifurcations do not require stability calculations to be detected.

4.2. Discussion

As shown in figure 1, the fundamental mode is stable beyond the state $b_1^{(1)}$, $\langle j \rangle \gtrsim 469\,\mathrm{A\,m^{-2}}$, in the abnormal regime; in the current range between states $b_1^{(3)}$ and $b_1^{(2)}$, $182\,\mathrm{A\,m^{-2}} \lesssim \langle j \rangle \lesssim 330\,\mathrm{A\,m^{-2}}$, in the normal regime; and before state $a^{(4)}$, $\langle j \rangle \lesssim 36\,\mathrm{mA\,m^{-2}}$, in the Townsend regime.

The state $b_1^{(1)}$ is very close to the point of minimum of the CVC. In other words, the whole abnormal discharge except for a very narrow section remains stable. If current in the abnormal discharge is reduced to a value below $469\,\mathrm{A\,m^{-2}}$, the loss of stability may occur in two ways, depending on whether the value of current after reduction is below, or above, $466\,\mathrm{A\,m^{-2}}$. If the former is the case, a likely scenario is a monotonic transition to the first or a higher-order steady-state 3D mode. If the current density is reduced to a value within the range $466\,\mathrm{A\,m^{-2}} \lesssim \langle j \rangle \lesssim 469\,\mathrm{A\,m^{-2}}$, the loss of stability occurs through perturbations oscillating in time. Since the latter current range is very narrow (in fact, its width is close to the limit of accuracy of the computations), the first possibility is more likely, and indeed there seem to be no indications in the literature of oscillations in the course of transition from the abnormal discharge to the steady-state normal mode or to a steady-state mode with multiple spots. On the other hand, it is of interest to perform experiments on this transition with a fine current step in order to try to detect oscillations.

The conclusion that the axially symmetric normal mode is stable in a rather wide current range, from 182 to $330\,\mathrm{A\,m^{-2}}$, is theoretically very interesting: while in most cases normal spots are attached to the edge of a (circular) cathode (e.g. the lower-right and adjacent images in figure 3 in [5]), the linear stability theory predicts that a stable normal mode with the spot at the centre can exist in microdischarges. It is of interest to check this prediction experimentally.

If current in the Townsend discharge is increased to a value exceeding $36\,\mathrm{mA\,m^{-2}}$, the loss of stability may occur in two ways, depending on whether the current after the increase is below, or above, $40\,\mathrm{mA\,m^{-2}}$. If the former is the case, the loss of stability is oscillatory. If the latter is the case, the perturbations grow monotonically in time. On the other hand, it is natural to expect that there are no stable steady-state solutions in the current range in question; note that the first 3D solution branches off at the state $b_1^{(4)}$, i.e. at considerably higher currents, and in any case an initial section of this solution is unstable (against oscillatory perturbations of the same mode that is growing at all states of the fundamental mode between $a^{(1)}$ and $a^{(4)}$, in particular, at the state $b_1^{(4)}$). Then the monotonic growth of perturbations which occurs on the linear stage in the case where the increased current exceeds $40\,\mathrm{mA\,m^{-2}}$ will give way to oscillations on the nonlinear stage.

It is well known that oscillations develop under certain conditions in the course of transition from the stable Townsend discharge at low currents to the normal mode of glow discharge; e.g. [20–22, 42, 45–48] and references therein. Although a quantitative comparison requires further work (in particular, effect of the external circuit needs to be taken into account), we note that small oscillations are observed in the experiment for currents slightly exceeding the limit of stability of Townsend discharge and nonlinear oscillations are observed for higher currents [45], in agreement with the above-described results of the linear stability theory.

It is of interest to consider also the case where ions and electrons coming to the wall are reflected rather than absorbed and the second boundary condition in (9) is replaced by zero derivatives. In this case, the fundamental mode of the discharge becomes 1D: all the parameters vary only in the axial direction, i.e. $F = F(z)$. This is the 1D form of glow discharge, to which the classical von Engel and Steenbeck theory refers (e.g. [1]). The pattern of stability of this mode is the simplest and the easiest to understand. For this reason, stability of the 1D glow discharge has been investigated as well. Skipping for brevity details (see [49]), we only note the following.

The independent variables in the eigenvalue problem of section 2.3 can be separated in this case and the eigenvalue problem that needs to be solved numerically is 1D. The pattern of changes in stability of the 1D fundamental mode against 2D and 3D perturbations is the same as that of the 2D fundamental mode against 3D perturbations between states $b_1^{(1)}$ and $b_1^{(2)}$, seen in the inset in figure 1. In fact, this pattern is typical for bistable nonlinear dissipative systems. Also detected in the modelling was a change in stability of the 1D fundamental mode against 1D oscillatory perturbations, which is an analogue of the change in stability of the 2D fundamental mode against 2D oscillatory perturbations occurring at the state $a^{(1)}$ in figure 1.

Changes in stability occurring at states $a^{(2)}$, $a^{(3)}$, $a^{(4)}$, $b_1^{(3)}$, $b_1^{(4)}$ in figure 1 have no analogues in the case of 1D fundamental mode. The changes in stability occurring at $a^{(2)}$ and $a^{(3)}$ can be understood with the use of the general theory [19]: the theory predicts the existence of a mode of real perturbations which possess the same (axial) symmetry as the discharge itself and switch between decay and growth at every turning point. The return to decay of the 2D oscillatory perturbations occurring at the state $a^{(4)}$ corresponds to the experiment (a stable Townsend discharge can be observed if the current is low enough). Since this return does not occur in the modelling for reflecting wall, one can conclude that the instability against oscillatory perturbations of the same symmetry is suppressed at low currents by losses of charged particles due to their diffusion to the wall. The changes in stability against 3D perturbations with the azimuthal period of 2π occurring at states $b_1^{(3)}$ and $b_1^{(4)}$ are similar to those occurring at states $b_1^{(1)}$ and $b_1^{(2)}$. Although these changes could have hardly been expected in advance, their presence is not particularly surprising.

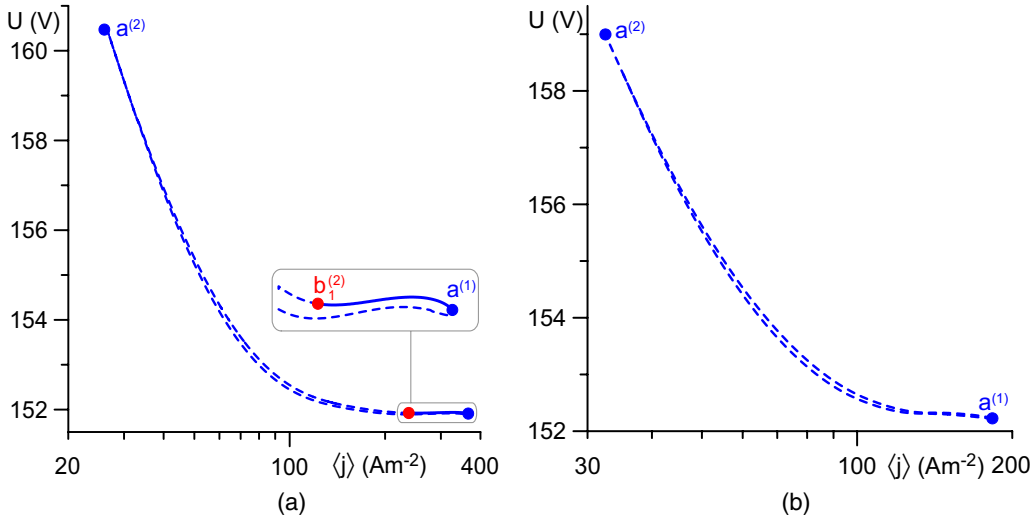

Figure 3. CVCs of the first (a) and second (b) non-fundamental axially symmetric steady-state modes. Solid: stable section. Dashed: unstable sections. Circles: points of change in stability against one of perturbation modes.

The pattern of changes in stability of the fundamental mode in the case of glow discharge, shown in figure 1, is significantly more complex than that in the case of arc cathodes [23, 24]: only switching of 3D perturbation modes from decay to growth in the vicinity of the point of minimum of the CVC, similar to that occurring between the states $b_1^{(1)}$ and $b_7^{(1)}$ in the inset in figure 1, exists in the case of arc cathodes. As mentioned above, this switching is typical for bistable nonlinear dissipative systems. Note that the perturbations do not return to decaying in the case of arc cathodes. However, if one takes into account that the near-cathode voltage in the arc discharge takes a finite value for low currents rather than infinitely high values as assumed in the theory [23, 24], then perturbations will return to decaying and this return will occur along exactly the same lines as that of perturbations of the fundamental mode of glow discharge between the states $b_7^{(2)}$ and $b_1^{(2)}$ in the inset in figure 1.

In order to compute multiple steady-state solutions describing different modes of stationary current transfer, one needs to have in advance an idea of what each solution looks like and in which current range it should be sought. For this reason, numerical calculation [17, 18] of each 2D or 3D steady-state mode branching from the 1D fundamental mode started in the vicinity of the corresponding bifurcation point. The employed procedure involved a numerical solution of the above-mentioned 1D eigenvalue problem for perturbations and was based on the following. If all perturbation modes with a given m are decaying at $\langle j\rangle = j_1$ and there is one real perturbation mode with a positive eigenvalue at a close value $\langle j\rangle = j_2$, then a steady-state bifurcation associated with this m occurs in the interval $[j_1, j_2]$. The latter is true also in cases where this perturbation mode switches from decay to growth through a Hopf bifurcation and becomes real after that. Therefore, one can start looking for a 3D steady-state solution with the azimuthal period of $2\pi/m$ (or for a 2D solution, if $m = 0$) in this interval without investigating details of bifurcations.

5. Stability of axially symmetric non-fundamental modes

In addition to the fundamental mode stability studied above, two other axially symmetric steady-state modes exist under the conditions considered. CVCs of these modes are shown in figure 3. Without going into details (see [17]), we note that each mode exists in a limited current range and represents a loop, i.e. is constituted by two branches separated by turning points designated $a^{(1)}$ and $a^{(2)}$. One of the modes, designated the first mode, exists in a wider current range than the second one. There are no self-intersections of the CVCs, so one can designate the two branches of each mode a low-voltage branch and a high-voltage branch, although in reality the discharge voltages corresponding to the two branches are very close.

For each steady-state mode, a mode exists of real axially symmetric perturbations with the eigenvalue vanishing at each of the turning points $a^{(1)}$ and $a^{(2)}$; a result in agreement with the general theory [19]. For both non-fundamental steady-state modes these perturbations are growing on the low-voltage branch and are decaying on the high-voltage branch.

Switching of 3D perturbations with several values of m between decay and growth is shown in figure 4 for the first non-fundamental 2D steady-state mode. Growing perturbation modes, all of them real, have been detected for m up to 33. (More precisely, one growing perturbation mode was detected for each $m = 4, 5, \ldots, 33$. Two growing perturbation modes were detected for each $m = 1, 2, 3$; however, the window of growth of one of these modes is positioned inside the window of growth of the other, therefore the former mode is irrelevant and excluded from the following discussion.) Each one of these perturbation modes switches between decay and growth at two states. For most m, one of these states (designated $b_m^{(1)}$) belongs to the low-voltage branch and the other ($b_m^{(2)}$) to the high-voltage branch. It was found that for every m of this group the perturbation mode in question is decaying on the section $b_m^{(1)}a^{(1)}b_m^{(2)}$ and growing on $b_m^{(1)}a^{(2)}b_m^{(2)}$. For others m (e.g. for $m = 33$ as seen in figure 4), both points belong to the high-voltage branch. It was found that for every m of this group the

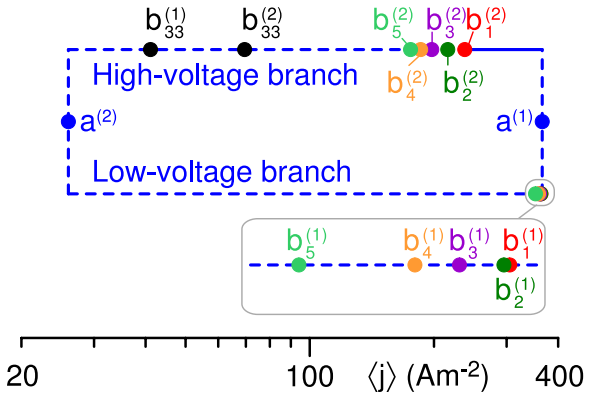

Figure 4. Points of change in stability of the first non-fundamental axially symmetric steady-state mode against some of perturbation modes. Solid: stable section. Dashed: unstable sections.

perturbation mode in question is growing on the section of the high-voltage branch limited by the states $b_m^{(1)}$ and $b_m^{(2)}$ and is decaying at all other states.

One can conclude that the first axially symmetric non-fundamental steady-state mode is stable on the high-voltage branch between states $b_1^{(2)}$ and $a^{(1)}$, as shown in figure 3(*a*). This is in contrast to what has been found for arc cathodes, where this mode is always unstable [24]. The current range corresponding to the section $b_1^{(2)}a^{(1)}$ is relatively wide, $238\,\mathrm{A\,m^{-2}} \lesssim \langle j \rangle \lesssim 366\,\mathrm{A\,m^{-2}}$. Therefore, a pattern with an interior ring spot, which is associated with this mode [17], in principle can be observed in the experiment.

In the case of the second axially symmetric non-fundamental steady-state mode, there is, in addition to the above-described 2D perturbations with the eigenvalue vanishing at the turning points, another mode of growing 2D perturbations, and these perturbations, which are real as well, grow at all states. In addition, there are several modes of real 3D perturbations that grow at all states. The conclusion is that the second axially symmetric non-fundamental steady-state mode, which is associated with a pattern with a spot at the centre and an interior ring spot [17], is always unstable.

6. Summary and concluding remarks

Main features of stability of different axially symmetric modes of current transfer in dc glow discharges were investigated in the framework of the linear stability theory with the use of Comsol Multiphysics software, considering as an example conditions of microdischarges in xenon.

Both real and complex eigenvalues have been detected, meaning that perturbations can vary with time both monotonically and with oscillations. The fundamental mode of axially symmetric glow discharge is stable when it operates in the abnormal regime. There is a rather wide window of stability on the axially symmetric normal discharge, which is characterized by a normal spot at the centre of the cathode. The subnormal discharge is unstable under the considered conditions. The Townsend discharge is stable at low currents.

Loss of stability of the abnormal discharge in the vicinity of the point of minimum of the CVC and loss of stability of the Townsend discharge with increasing current develop in a general case in different ways: monotonically in time and with oscillations, respectively. This conforms to the well-known experimental facts that the transition from the abnormal discharge to the normal discharge or to a discharge with a multiple-spot pattern occurs without oscillations of the luminosity of the cathode or of the discharge voltage, while the transition from the stable Townsend discharge to the normal glow discharge can be accompanied by oscillations. On the other hand, the linear stability theory predicts that oscillations under conditions of microdischarges can occur also in the transition from the abnormal discharge to the normal discharge or to a discharge with a spot pattern, however in a very narrow current range. It is of interest to study these transitions experimentally with a fine current step in order to try to detect the oscillations.

Calculations of stability of the two axially symmetric non-fundamental steady-state modes which exist under the considered conditions in addition to the fundamental mode revealed that there is a relatively wide stability window on the first mode, while the second mode is unstable.

It is sometimes assumed, by analogy with nonlinear electric circuits with inductance, that a gas discharge with a negative differential resistance is stable provided that the ballast is high enough and the total differential resistance of the system is positive. A discussion of this conjecture in the context of stability of current transfer to high-pressure arc cathodes and of glow discharges is given in [49].

The question of existence of stable steady-state axially symmetric self-organized patterns in circular domains is of considerable theoretical interest; see, e.g., discussion in [50]. As far as gas discharges are concerned, axially symmetric self-organized patterns have been observed, in particular, on anodes of glow discharge [51, 52] and in dielectric barrier discharge [50]. It seems that such patterns have been observed also on cathodes of microdischarges in Xe; the upper-left image in figure 3 of [5] and the middle image in figure 4 of [9]. Since, according to the above, axially symmetric self-organized steady-state patterns on cathodes of microdischarges in Xe may be also theoretically stable, it would be very interesting to address this question by means of special experiments.

In general, results given by the linear stability theory confirm intuitive concepts developed in the literature and conform to the experiment. On the other hand, the theory provides suggestions for further experiments.

Modelling of this work has been performed with account of the simplest mechanisms of glow discharges, which are charge separation, ionization, recombination, drift and diffusion of charged particles, and with electron transport and kinetic coefficients evaluated in the local approximation. This is in part justified by successful application of this approach to modelling of self-organization in DBDs [28–31] and dc glow discharges [17, 18] and of formation and propagation of filamentary plasma arrays in high-power microwave breakdown at atmospheric pressure [32, 33], and also by the fact that an account of a more realistic chemistry and non-locality of electron coefficients does not affect steady-state solutions qualitatively [34]. Nevertheless, it is desirable to

take a more realistic chemistry and non-locality of electron coefficients into account also in the investigation of stability. Another possible direction of future work is investigation of stability of 3D steady-state modes with multiple spots, observed in the experiments [5–9].

Acknowledgments

The work was performed within activities of the project PTDC/FIS/68609/2006 *Cathode spots in high-pressure dc gas discharges: self-organization phenomena* of FCT, POCI 2010 and FEDER and of the project *Centro de Ciências Matemáticas* of FCT, POCTI-219 and FEDER. P G C Almeida and M J Faria appreciate PhD fellowships from FCT, grants SFRH/BD/30598/2006 and SFRH/BD/35883/2007.

References

[1] Raizer Yu P 1991 *Gas Discharge Physics* (Berlin: Springer)
[2] Korolev Yu D, Rabotkin V G and Filonov A G 1979 *High Temp.* **17** 181–3
[3] Bystrov S A, Lushchikova A M, Mazalov D A, Pal A F, Starostin A N, Taran M D, Taran T V and Filippov A V 1994 *J. Phys. D: Appl. Phys.* **27** 273–79
[4] Arkhipenko V, Kirillov A, Callegari T, Safronau Y and Simonchik L 2009 *IEEE Trans. Plasma. Sci.* **37** 740–9
[5] Schoenbach K H, Moselhy M and Shi W 2004 *Plasma Sources Sci. Technol.* **13** 177–85
[6] Moselhy M and Schoenbach K H 2004 *J. Appl. Phys.* **95** 1642–9
[7] Takano N and Schoenbach K H 2006 *Plasma Sources Sci. Technol.* **15** S109–17
[8] Zhu W, Takano N, Schoenbach K H, Guru D, McLaren J, Heberlein J, May R and Cooper J R 2007 *J. Phys. D: Appl. Phys.* **40** 3896–906
[9] Lee B J, Biborosch D L, Frank K and Mares L 2008 *J. Optoelectron. Adv. Mater.* **10** 1972–5
[10] Thouret W, Weizel W and Günther P 1951 *Z. Phys.* **130** 621–31
[11] Olsen H N 1963 *J. Quant. Spectrosc. Radiat. Transfer* **3** 305–33
[12] Benilov M S, Cunha M D and Faria M J 2009 *J. Phys. D: Appl. Phys.* **42** 145205
[13] Bade W L and Yos J M 1963 *Theoretical and Experimental Investigation of Arc Plasma-Generation Technology. Part II, Vol. 1: A Theoretical and Experimental Study of Thermionic Arc Cathodes. Technical Report No. ASD-TDR-62-729* (Wilmington, MA: Avco Corporation)
[14] Benilov M S and Pisannaya N V 1988 *Sov. Phys.—Tech. Phys.* **33** 1260–66
[15] Benilov M S 1988 *Sov. Phys.—Tech. Phys.* **33** 1267–70
[16] Benilov M S 2008 *J. Phys. D: Appl. Phys.* **41** 144001
[17] Almeida P G C, Benilov M S and Faria M J 2010 *Plasma Sources Sci. Technol.* **19** 025019
[18] Almeida P G C, Benilov M S and Faria M J 2011 *IEEE Trans. Plasma Sci.* **39**
[19] Almeida P G C, Benilov M S, Cunha M D and Faria M J 2009 *J. Phys. D: Appl. Phys.* **42** 194010
[20] Melekhin V N and Naumov N Yu 1984 *Sov. Phys.—Tech. Phys.* **29** 888–92
[21] Phelps A V, Petrović Z Lj and Jelenković B M 1993 *Phys. Rev.* E **47** 2825–38
[22] Kaganovich I D, Fedotov M A and Tsendin L D 1994 *Tech. Phys.* **39** 241–6
[23] Benilov M S 2007 *J. Phys. D: Appl. Phys.* **40** 1376–93
[24] Benilov M S and Faria M J 2007 *J. Phys. D: Appl. Phys.* **40** 5083–97
[25] Velikhov E P, Kovalev A S and Rakhimov A T 1987 *Physical Phenomena in a Gas Discharge Plasma* (Moscow: Nauka) (in Russian)
[26] Koch B P, Goepp N and Bruhn B 1997 *Phys. Rev.* E **56** 2118–29
see also Koch B P, Goepp N and Bruhn B 2000 *Phys. Rev.* E **62** 1455 (erratum)
[27] Bruhn B, Richter A and May B 2008 *Phys. Plasmas* **15** 053505
[28] Brauer I, Punset C, Purwins H G and Boeuf J 1999 *J. Appl. Phys.* **85** 7569–72
[29] Stollenwerk L, Amiranashvili Sh, Boeuf J P and Purwins H G 2006 *Phys. Rev. Lett.* **96** 255001
[30] Bernecker B, Callegari T, Blanco S, Fournier R and Boeuf J P 2009 *Eur. Phys. J. Appl. Phys.* **47** 22808
[31] Bernecker B, Callegari T and Boeuf J P 2010 Pattern formation in dielectric barrier discharges *Proc. 12th HAKONE (Bratislava, September 2010)* ed J Országh *et al* (Bratislava: Soceity for Plasma Research and Applications, Library and Publishing Centre CU) ISBN 978-80-89186-72-3 pp 19–30
[32] Boeuf J P, Chaudhury B and Zhu G Q 2010 *Phys. Rev. Lett.* **104** 015002
[33] Chaudhury B, Boeuf J P and Zhu G Q 2010 *Phys. Plasmas* **17** 123505
[34] Almeida P G C 2011 Investigation of modes of current transfer in dc glow and arc discharges *PhD Thesis* Universidade da Madeira
[35] Boeuf J P, Pitchford L C and Schoenbach K H 2005 *Appl. Phys. Lett.* **86** 071501
[36] Muñoz-Serrano E, Hagelaar G, Callegari Th, Boeuf J P and Pitchford L C 2006 *Plasma Phys. Control. Fusion* **48** B391
[37] Makasheva K, Muñoz-Serrano E, Hagelaar G, Boeuf J P and Pitchford L C 2007 *Plasma Phys. Control. Fusion* **49** B233
[38] Deconinck T and Raja L L 2009 *Plasma Processes Polym.* **6** 335–46
[39] Zhang X, Wang X, Liu F and Lu Y 2009 *IEEE Trans. Plasma. Sci.* **37** 2055–60
[40] He S, Ouyang J, He F and Li S 2011 *Phys. Plasmas* **18** 032102
[41] Hagelaar G J M, de Hoog F J and Kroesen G M W 2000 *Phys. Rev.* E **62** 1452–4
[42] Kolobov V I and Fiala A 1994 *Phys. Rev.* E **50** 3018–32
[43] Punset C, Boeuf J P and Pitchford L C 1998 *J. Appl. Phys.* **83** 1884–97
[44] Benilov M S and Faria M J 2008 Investigation of stability of current transfer to thermionic cathodes *Proc. European COMSOL Conf. (Hannover, Germany, 4–6 November 2008)* (COMSOL) ISBN 978-0-9766792-3-3
[45] Melekhin V N, Naumov N Yu and Tkachenko N P 1987 *Sov. Phys.—Tech. Phys.* **32** 274
[46] Kudryavtsev A A and Tsendin L D 2002 *Tech. Phys. Lett.* **28** 1036–9
[47] Arslanbekov R R and Kolobov V I 2003 *J. Phys. D: Appl. Phys.* **36** 2986–94
[48] Raizer Yu P, Gurevich E L and Mokrov M S 2006 *Tech. Phys.* **51** 185–97
[49] Faria M J 2011 Stability and bifurcations of modes of current transfer to cathodes of dc gas discharges *PhD Thesis* Universidade da Madeira
[50] Gurevich E L, Zanin A L, Moskalenko A S and Purwins H G 2003 *Phys. Rev. Lett.* **91** 154501
[51] Thomas C H and Duffendack O S 1930 *Phys. Rev.* **35** 72–91
[52] Müller K G 1988 *Phys. Rev.* A **37** 4836–45